Excited-State Properties of a Photochromic Spirooxazine: Double Pathways for Both Fluorescence Emission and Camphorquinone-Sensitized Reaction

Maria Rosaria di Nunzio, Aldo Romani, and Gianna Favaro*

Università di Perugia, Dipartimento di Chimica, 06123 Perugia, Italy

Received: May 21, 2009; Revised Manuscript Received: July 15, 2009

In this article, we report a study on the singlet and triplet excited-state properties of a spirooxazine (1,3-dihydro-3,3-dimethyl-1-isobutyl-6′-(2,3-dihydro-1*H*-indol-1-yl)spiro[2*H*-indole-2,3′−3*H*-naphtho[2,1-*b*][1,4]oxazine]). The singlet state of this molecule is photoreactive: upon UV light stimulation, it produces a colored merocyanine that thermally reverts to the starting compound. A double-way radiative relaxation path was found for singlet-state excitation. Experimental observations on the absorption and fluorescence spectra were in excellent agreement with TD-DFT calculations for the singlet state. The triplet state, which could not be directly populated by intersystem crossing from the singlet, when reached by energy transfer from a suitable sensitizer (camphorquinone), yielded the colored merocyanine with quantum yield close to unity. However, the donor/acceptor interaction also originated a new photochromic system as a consequence of the competition of hydrogen abstraction with energy transfer in the interplay of the sensitizer with the substrate. The newly produced photochrome was structurally, spectrally, and photochemically characterized. It exhibited excellent colorability in both directly excited and triplet-sensitized photoreactions by virtue of high photoreaction quantum yield and rather slow bleaching rate of the colored form but also underwent significant degradation in the presence of oxygen that led to the destruction of the photochromic functionality.

1. Introduction

Spirooxazines are by far the most widely investigated photochromic compounds since the pioneering work by Fisher and Hirshberg.[1,2] Later, many photochromic molecules belonging to this class[3−5] were synthesized in academic and industrial research laboratories in the attempt to meet some demanding requirements, such as suitable response time, thermal stability, and fatigue resistance, to be promising for technological applications. All photochromic processes pass through electronically excited states. An in-depth understanding of the excited-state properties and the effect of perturbations induced by the chemical environment, the solvent, and the temperature may help in the design of new photochromic molecules for smart materials and in choosing the most suitable for each specific application.

In this article, we focused attention on a commercial photochromic spirooxazine, 1,3-dihydro-3,3-dimethyl-1-isobutyl-6′-(2,3-dihydro-1*H*-indol-1-yl)spiro[2*H*-indole-2,3′−3*H*-naphtho[2,1-*b*][1,4] oxazine (SO), with the aim of gaining more insight into the properties of the excited states by investigating the dependence of absorption and emission spectra on environmental and excitation conditions.

The photochromic reaction of this molecule, which has been previously investigated in acetonitrile (ACN) solution,[6] implies photocleavage of the spiro-bond of SO, which absorbs in the UV, leading to the formation of an open merocyanine structure (PM), which is deeply colored, with a quantum yield of 0.24 (λ_{exc} = 355 nm, Scheme 1). The reaction is thermally reversible (k = 1.35 s^{-1} in ACN at 298 K).
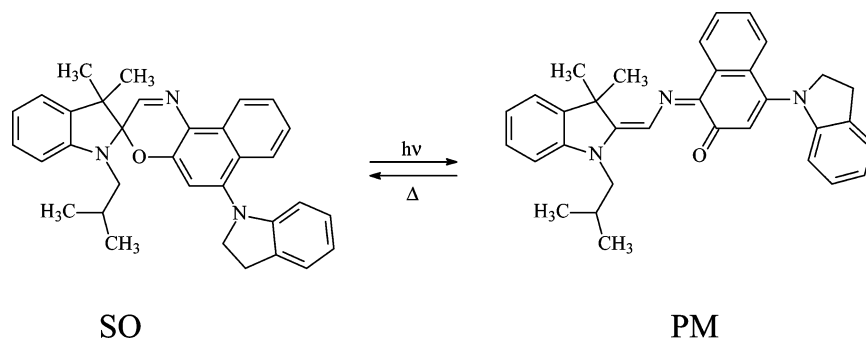
Compared with other SOs, this compound showed peculiar properties, which could be potentially interesting for applications, such as absorption spectra of both the colored and colorless forms shifted toward the red (thus allowing activation by solar light) and good photocolorability and thermocolorability. Furthermore, it emitted fluorescence with quantum yield that was exciting-wavelength-dependent.[6] Preliminary observations had shown some peculiar effects of the solvent on the absorption and fluorescence properties of this compound that stimulated a more in-depth investigation of the properties of the excited states through steady-state and time-resolved absorption measurements, fluorescence emission, TD-DFT calculations, and triplet-state sensitization of the photochromic reaction. Triplet-state photosensitizers have often been used to provide information on excited-state properties and photoreaction mechanisms[7] and are tools for promoting and orienting photochemical reactions.[8] Even in nature, many photoactivated processes occur via energy transfer mechanisms. When applied to photochromic compounds, photosensitization plays the role of extending toward the visible the λ-range for producing the colored merocyanine form, which may represent an important goal from an applicative point of view. Triplet−triplet energy transfer experiments from suitable donors to spirocompounds have demonstrated that a triplet pathway leading to merocyanine formation is available and that the efficiency of photocoloration via triplet-state sensitization is often close to unity.[9−17] Here we used camphorquinone (CQ) as a triplet photosensitizer because of its absorption spectral characteristics that are suitable to be combined with those of SO, high intersystem crossing yield ($\Phi_{ISC} \approx 1$) and long triplet lifetime ($\tau_T \approx 200−400\ \mu s$) in solution.[18] Moreover, CQ represents a rare example of room-temperature phosphorescent molecule; therein energy transfer processes from the triplet state can be easily followed by the phosphorescence quenching. As previously reported, CQ can work as an efficient triplet sensitizer for spiranic photochromic compounds.[12,15,16,18]

The direct electronic excitation of spirocompounds generally results in reaction from the singlet state because the photoprocess

* Corresponding author. Tel: +39 075 5855573. Fax: +39 075 5855598. E-mail: favaro@unipg.it.

Photochromic Spirooxazine Excited-State Properties

J. Phys. Chem. A, Vol. 113, No. 34, 2009 **9425**

SCHEME 1: Thermoreversible Photochromic Reaction of SO

SO   PM

is fast and the intersystem crossing to the triplet is scarcely efficient. However, for some nitrosubstituted molecules, a substantial contribution of triplet mechanism to the direct photoreaction was found;[9,13] in a few other cases, the contribution, even if present, was hardly detectable.[19]

2. Experimental Methods

2.1. Materials. Spirooxazine was purchased from James Robinson Ltd. and was carefully purified by HPLC. Camphorquinone (1,7,7-trimethylbicyclo[2.2.1]heptane-2,3-dione]), Aldrich, was crystallized from cyclohexane and then sublimated in vacuo. The solvents used, ACN, methylcyclohexane (MCH), benzene (Bz), diethylether (EE), and dimethyl sulfoxide (DMSO), were reagent grade Fluka products.

2.2. Equipment. The absorption spectra were recorded using a HP 8453 diode-array spectrophotometer and a double-beam Perkin-Elmer Lambda 800 UV−visible spectrophotometer. Corrected emission spectra were taken using a Spex Fluorolog-2 FL 112 spectrofluorimeter or an Eclipse Varian spectrofluorimeter.

For purifications and separations, a HPLC system, equipped with Waters 600 pump and controller, 2487 dual λ absorbance, and 996 photodiode array detector, was used. An ACN/water mixture (90/10 v/v) was used as eluent. An Altima C18 column was chosen as the stationary phase.

For laser flash photolysis measurements, the third harmonic ($\lambda = 355$ nm) from a Continuum Surelite Nd/YAG laser was used with energy less than 5 mJ per pulse and time resolution of about 20 ns. Details are reported elsewhere.[20]

For structural investigations, NMR spectra were taken using a Bruker Avance DRX 400 spectrometer.

Mass spectrometry analyses were carried out on an Agilent 6890N GC/5973 inert MS system equipped with a JWS-MS column (30 m × 0.25 mm) using Helium as the gas carrier at a flow rate of 1.1 mL/min and injector temperature of 330 °C.

2.3. Measurement Conditions. *2.3.1. Emission Quantum Yield Measurements.* To measure emission quantum yields, we compared corrected areas of the standard (anthracene in ethanol $\Phi_F = 0.27 \pm 0.03$)[21] and the sample ($A = 0.11$ to 0.01) emissions. When necessary, the signals of the solvent contribution were subtracted and corrected for self-absorption.

2.3.2. Phosphorescence Quenching Measurements. In an oxygen-free solution obtained by nitrogen bubbling, the contribution from phosphorescence to the total room-temperature emission intensity of CQ is comparable to that from fluorescence; however, when recording the emission at delayed times, only phosphorescence was detected. Phosphorescence quenching measurements were performed in solutions containing the sensitizer ([CQ] = 3.54×10^{-3} mol dm^{-3}) and varying amounts of the quencher ([SO] = 4×10^{-7} to 1.6×10^{-6} mol dm^{-3}).

2.3.3. Quantum Yield Measurements of Photosensitized Reaction. The photokinetic measurements were carried out under continuous irradiation in ACN solutions deaerated by bubbling with pure nitrogen. The light exposure ($\lambda_{exc} = 450$ nm) of the sample (1 cm path cell, 1 cm^3 of solution) was carried out in the spectrophotometer holder at a right angle to the analysis beam at $T = 270$ K (controlled by an Oxford Instruments cryostat). A 125 W Xe lamp, coupled to a Jobin-Yvon H10 UV monochromator, was used for irradiation. The SO and SOX concentrations were on the order of 4×10^{-5} mol dm^{-3} and that of the sensitizer was 3.8×10^{-3} mol dm^{-3}, corresponding to 0.089 absorbance at the excitation wavelength. The increase in the PM and PMX absorbances under stationary irradiation, was followed at the absorption maximum wavelength of the colored forms, 600 and 616 nm, respectively. The rate parameters of the ring-closure reaction (first-order kinetics) were spectrophotometrically determined following the disappearance of the colored form in the visible region after having shut down the irradiating source. Because of the critical deaeration conditions, sensitized reaction quantum yields are affected by a greater uncertainty than direct photoreactions, which can be estimated to be around 20−30%.

2.3.4. Production, Purification, and Identification of SOX. To obtain pure SOX, a concentrated ACN solution of SO (1.07 × 10^{-4} mol dm^{-3}) and CQ (7.22 × 10^{-2} mol dm^{-3}) was irradiated with 436 nm light, selected from a medium pressure 250W Hg lamp (Applied Photophysics LTD) by an Oriel interferential filter. Before and during the whole time of irradiation (∼6 h), the solution was deaerated by bubbling with pure nitrogen. The irradiation time was suitable for producing a high SOX concentration (as controlled by spectrophotometry) before degradation. Then, volumes of irradiated solutions ranging from 250 to 500 μL were injected on top of the chromatographic column; SOX was separated from the mixture, having a different retention time (∼17 min) with respect to CQ (∼3 min), residual unreacted SO (∼20 min), and minor byproducts (5−12 min). The acetonitrile/water mixture was removed from the eluate using a rotary evaporator; the dried pure SOX was stored in the dark.

For the identification of SOX structure, NMR and mass spectrometry analyses on pure samples of SOX and SO were carried out and compared.

For NMR structural analyses, spectra were taken in C$_6$D$_6$ and CD$_2$Cl$_2$ at room temperature. Both spirooxazines were characterized by 1D ^{1}H and ^{13}C NMR experiments. Bidimensional homonuclear shift correlation (COSY) and bidimensional nuclear Overhauser effect (NOESY) were also performed to give a clearer understanding of the SOX structure. Comparison of the results for the two molecules indicated that their spectra are quite similar, with the exception of δ_H and δ_C values for the

two positions of the methylene groups of the indoline 6′-substituent in SO. In SO, two multiplet signals (δ_H = 3.37 and 2.66 ppm) were assigned to the hydrogen atoms and residual frequencies (δ_C = 54.4 and 36.3 ppm) to the carbon atoms of methylene groups. In SOX, the signals shifted toward higher frequencies in the region of aromatic and nonaliphatic compounds (δ_H = 7.18 and 7.72; δ_C = 120.2 and 120.7) because of the formation of a double bond between the two carbon atoms. This suggested that an indole group replaces the indoline 6′-substituent in SOX.

For mass spectrometric analyses, the pure compounds were dissolved in pyridine. SO was characterized by a retention time of 16 min: the mass-to-charge ratio computed was 487.40 *m/z* (SO molecular mass = 487.64). Because of the high operation temperature, SO underwent several fragmentations: at least four secondary species were detected in the gas chromatogram in addition the SO peak. Analogous results were obtained for SOX, with the difference that the mass-to-charge ratio (485.3 *m/z*) was 2 *m/z* lower than that for SO, corresponding to the loss of two H atoms. This is in agreement with the NMR indication that indole replaces indoline as the 6′-substituent in SOX.

2.4. Computational Methods. The semiempirical PM3/AM1 method was used to compute fully optimized ground-state geometries, and AM1 with configuration interaction was used to simulate the absorption spectra.

TD-DFT (time-dependent density functional theory) calculations were carried out using the ADF (Amsterdam density functional) 2007.01 program package.[22] Geometry optimization and ground-state electronic structure calculations were performed using the Vosko−Wilk−Nusair (VWN) local density approximation (LDA) functional[23] plus the Becke−Perdew-generalized (BP) gradient approximation (GGA).[24] Structure optimizations were performed using no constraints. Excitation energies were calculated using ordinary TD-DFT,[25] where the same GGA as that in the DFT calculations was used for the XC potential. The DFT and TD-DFT calculations employed the all-electron ADF QZ4P basis set.

3. Results and Discussion

3.1. Singlet State. *3.1.1. Absorption Spectrum of SO.* The compound under study exhibited dependence of the absorption and emission spectra on the solvent, concentration, and temperature. On the basis of the AM1 calculation, the lowest-energy absorption band detectable in the SO spectrum (λ_{max} = 386 nm in ACN) at the usual spectrophotometric concentration ($\sim 10^{-5}$ mol dm^{-3}) was assigned to excitation localized in the naphthooxazine moiety (Figure 1). This transition was scarcely affected by the solvent; a positive solvatochromic effect (red spectral shift with increasing of the $E_T(30)$ solvent parameter[26]) in accord with the π,π^* nature of the transition could hardly be detected.

Calculated and experimental spectra are in good agreement; however, when more concentrated ($\sim 5 \times 10^{-3}$ mol dm^{-3}) SO solutions were examined, a weak intensity absorption band appeared around 480 nm ($\varepsilon \approx 180$ dm^3 mol^{-1} cm^{-1} in ACN). There is no doubt that this absorption belongs to the SO molecule and not to some impurity because it was detected in very carefully purified samples. Moreover, monochromatic irradiation on this band of a concentrated SO solution produced the same PM as that obtained by exciting into the other hypsochromic bands. It was assigned to a n,π^* transition, where an electron moves from the lone pair of the N atom of the 6′-indolyl substituent to the naphthooxazine moiety (intramolecular
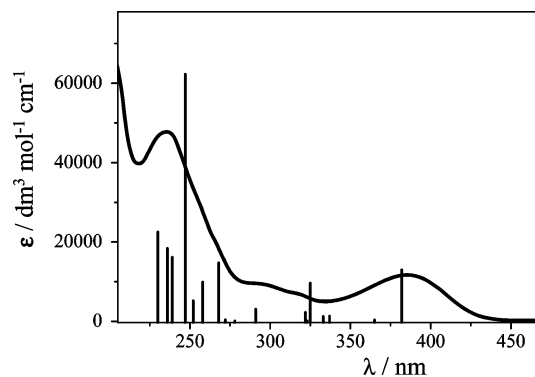

Figure 1. Oscillator strengths (vertical lines) calculated for SO compared with the absorption spectrum in 3MP using the approximate relationship, $f = (2 \times 10^{-5})\varepsilon$.
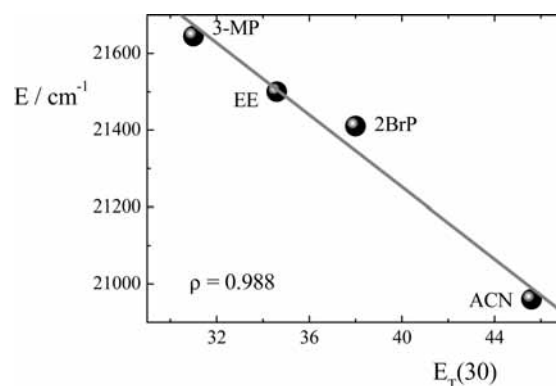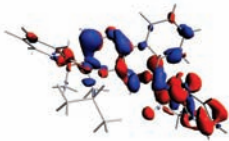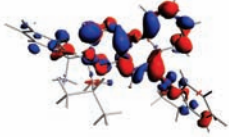

Figure 2. Solvatochromic effect on the lowest-energy (CT) absorption band of SO (legend: 3-MP, 3-methylpentane; EE, diethyl ether; 2BrP, 2-bromopropane; ACN, acetonitrile).

charge transfer (ICT) transition). This weak transition is undetectable in hydrogen-donating media, where the lone pair of the N atom is engaged in hydrogen bonding with the solvent. The ICT assignment is in agreement with the positive solvatochromic effect found experimentally (Figure 2) and is also supported by TD-DFT calculations (Table 1), where computed vertical absorption energies and electron density redistribution in the excited states are compared with the experimental spectroscopic data in ACN solution. There is an excellent agreement between theoretical and experimental energy values.

The five orbitals that are responsible for the appearance of the spectroscopic bands at 386 nm and ~480 nm in ACN solution are HOMO, LUMO, HOMO-1, HOMO-2, and LUMO+2. The HOMO receives contribution mainly from the N atom of the 6′-indolyl substituent, whereas the LUMO orbital is largely localized on the naphthooxazine moiety. In HOMO-2, the distribution of electronic density is close to that computed for HOMO. In HOMO-1 the main contribution comes from the indole moiety. A strong antibonding character was discovered for the LUMO+2 orbital, which lies over the whole molecular skeleton. According to the TD-DFT calculations, the weak absorption band observed around 480 nm is mainly derived from an ICT from the 6′-indolyl substituent to the naphthooxazine moiety, as foreseen on the basis of experimental data. The excited state calculated at 3.299 eV (378 nm) arises from the mixing of an ICT (44.2%) and a π,π^* transition (37%).

3.1.2. Absorption Spectrum of PM. The absorption maximum of the PM, produced under irradiation, ranges from 590 nm in a nonpolar solvent, diethyl ether (EE), to 612 nm in a polar hydrogen bonding solvent, ethanol, and therefore exhibits a positive solvatochromic shift in accord with its π,π^* character (Figure 3).

Photochromic Spirooxazine Excited-State Properties

J. Phys. Chem. A, Vol. 113, No. 34, 2009 **9427**

TABLE 1: Excitation Energies and Electronic Densities Computed for the Lowest Singlet State Transitions of SO Compared with the Experimental Spectral Data

transition character	transition density [a]	energy / eV (nm)	
		computed	ACN solution
HOMO → LUMO HOMO-1 → LUMO (ICT)		2.598 (477)	2.568 (483)
HOMO-2 → LUMO HOMO → LUMO+2 (ICT, π,π*)		3.299 (378)	3.213 (378)

[a] Electron density redistribution in the excited states. Red indicates a decrease and blue indicates an increase in electron density upon excitation.
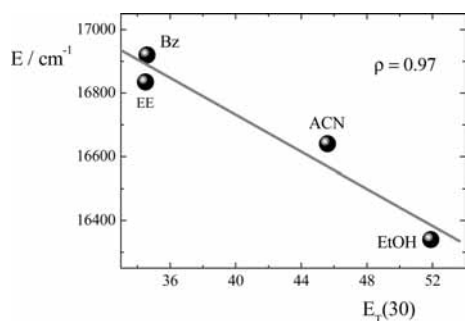

Figure 3. Solvatochromic effect on the colored band of the PM (legend: Bz, benzene; EE, diethyl ether; ACN, = acetonitrile; EtOH, ethanol).

Figure 4. Normalized absorption and fluorescence spectra of SO in various solvents.

Positive solvatochromism has been previously reported for most of the merocyanines because of the large contribution of weakly polar quinoid forms to the ground-state resonance hybrid,[27,28] with a few exceptions such as PMs derived from some 6-nitro-benzo-indolinospiropyrans that exhibit negative solvatochromic effect.[29] Changing the solvent from a polar to a nonpolar solvent also had the effect of making the thermally equilibrated PM undetectable. In fact, in a polar solvent, such as ACN, thermochromism was observed ($K_{equilibrium} = 2 \times 10^{-3}$)[6] because the transition state of the SO → PM ground-state reaction is stabilized by solvent polarity, thus lowering the energy barrier to the coloration process. In nonpolar solvents, thermochromism could hardly be detected for this compound as for other structurally related molecules.[28]

3.1.3. Fluorescence of SO. Depending on the solvent and the excitation wavelength, SO exhibited a dual fluorescence; one (F_A) is centered around 575 nm, and the other (F_B), especially evident in nonpolar solvents, is centered around 480 nm. Excitation in the π,π* transition (∼380 nm) invariably produces the F_A emission (Figure 4). Excitation spectra corresponded well enough to absorption spectra to ensure that observed emission was real and not due to impurities. The large separation between the absorption and fluorescence bands (∼8500 cm^{-1}) and the lack of mirror image symmetry observed for F_A demand that there is a significant configurational change between the ground-state geometry and that of the fluorescent singlet state.

Quantum yields of F_A, determined in three solvents at different excitation wavelengths, are reported in Table 2.
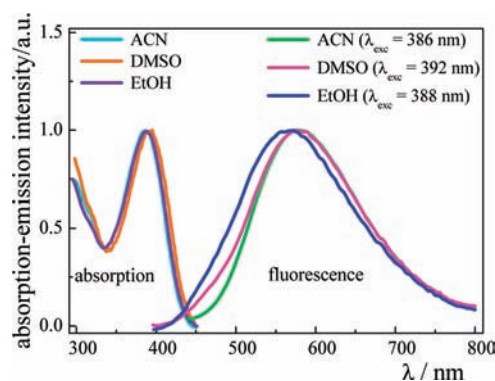
TABLE 2: F_A Quantum Yields (Φ_{FA}) Determined in Three Solvents at Various Excitation Wavelengths

solvent	ACN	DMSO	EtOH
$\lambda_{em(max)}$/nm	580	580	567
$\Phi_{FA} \times 10^3$ (λ_{exc}/nm)	10 (476)		
	30 (410)	37 (416)	6.1 (412)
	26 (386)	36 (392)	6.0 (388)
	24 (355)	37 (363)	5.9 (357)
	15 (316)	22 (320)	3.6 (318)
	11 (295)	14 (294)	2.9 (298)
	0.34 (235)		

From the table, it can be seen that Φ_{FA} is lower in ethanol, probably owing to competitive relaxation processes through vibrational modes of the H bond with the solvent. The exciting wavelength effect is similar in all of the solvents, as can be seen from the table, with Φ_{FA} being approximately constant with λ_{exc} around the absorption maximum, whereas it decreased when λ_{exc} was shifted to a higher-energy electronic transition.

In brief, solvent polarity and hydrogen-bonding ability determine the fluorescence behavior: in the polar and non-hydrogen-bonding ACN, only F_A was observed anywhere the excitation was carried out; in the nonpolar and non-hydrogen-bonding 3-MP, only F_B was observed anywhere the excitation occurred, and in solvents of intermediate polarities, both emissions were detected simultaneously (EE) and/or by changing the excitation wavelength (EtOH, Bz). Examples of the different behaviors in three solvents, ACN, Bz, and EE, are depicted in Figure 5.
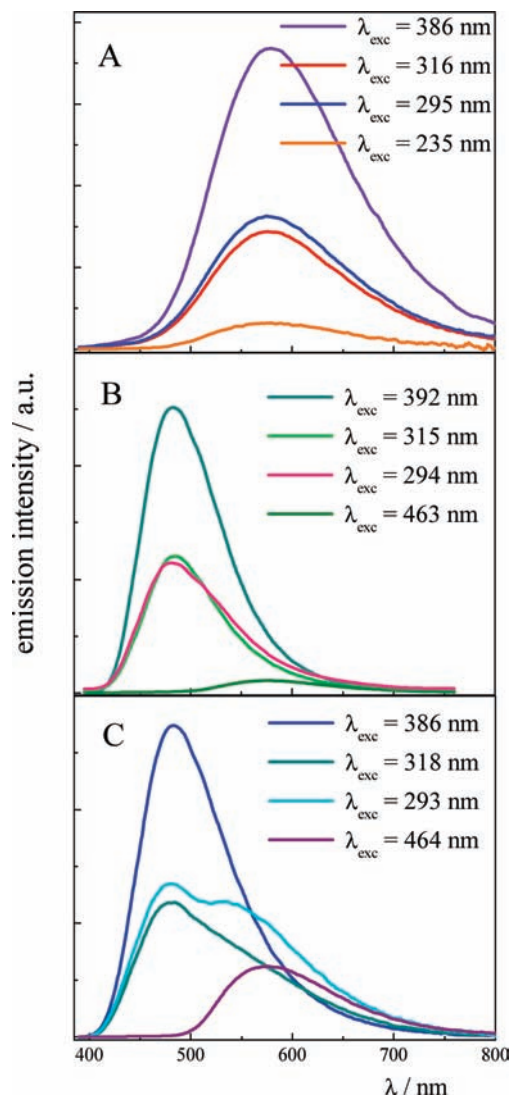
Figure 5. Emission spectra of SO in (A) ACN, (B) benzene, and (C) EE solutions excited at different wavelengths at room temperature.

Figure 6. Quenching of CQ phosphorescence by SO in ACN at room temperature ([CQ] = 1.31×10^{-3} mol dm^{-3}, [SO] = 3.1×10^{-7} to 1.4×10^{-6} mol dm^{-3}). Insert: Stern−Volmer plot for the quenching, eq 1.

3.2. Triplet State. Attempts to populate the triplet state by 355 nm laser excitation failed because irradiation yielded the merocyanine-colored form directly without any evidence of a triplet precursor, as also supported by the insensitivity of PM photoproduction to the presence or absence of oxygen. Therefore, to obtain information on the reactivity of the triplet state of SO and its role in the relaxation paths of electronically excited states, the triplet was populated by photosensitization. Camphorquinone (CQ) was selected as the photosensitizer, which allows irradiation to be carried out at a wavelength (450 nm) that the SO does not appreciably absorb. To test the efficiency of energy transfer (ET), we carried out quenching measurements of CQ phosphorescence by SO. The quenching efficiency of the sensitizer phosphorescence is illustrated in Figure 6. The data were treated according to the Stern−Volmer equation

$$I^0/I = 1 + k_{ET}\tau_{CQ}[SO] \qquad (1)$$

wherein I^0 and I are the phosphorescence intensities in the absence and in the presence of the quencher, respectively, k_{ET} is the rate coefficient for the sensitizer−quencher interaction, and τ_{CQ} (430 μs) is the triplet lifetime of the sensitizer. From the linear plot obtained (Figure 6, inset), $k_{ET} = (2.9 \pm 0.3) \times 10^9$ dm^3 mol^{-1} s^{-1} was determined, which is a rate close to that for a diffusion-controlled process. This value is in accord with those reported for structurally related photochromes interplaying with other donors, having triplet energy greater than 210 kJ mol^{-1}.[14]

The efficiency of triplet energy transfer from CQ indicates that the triplet-state energy of SO is lower than that of the sensitizer (210 kJ mol^{-1}).

3.2.1. Photosensitized Reaction: A Preliminary Experiment. We first probed the sensitized photoreaction by continuously irradiating with 450 nm light an ACN solution containing [CQ] = 3.54×10^{-3} mol dm^{-3} and [SO] = 3.44×10^{-5} mol dm^{-3}. This preliminary experimental run revealed the complex character of the donor(CQ)/quencher(SO) interaction, which was triggered by the sensitizer because it was the only molecular species absorbing the exciting light. (The CT transition of SO, which was undetectable under the experimental conditions used, cannot be responsible for any light absorption.) The spectral time evolution, under the experimental conditions adopted, is shown in Figure 7. During the first few seconds (ca. 20 s) of irradiation, the same photoproduct was detected, as obtained by direct reaction ($\lambda_{max} = 601$ nm).[6] Prolonging the irradiation, the color band slowly shifted toward longer wavelengths (λ_{max}

Double fluorescence emission is not uncommon for molecules containing electron donor and electron acceptor moieties linked by a formally single bond that can bring about an ICT process with the formation of a CT state.[30] Flexible molecules usually undergo significant structural modifications upon intramolecular electron migration. Different models have been proposed to explain the presence of double fluorescence, which is governed by the solvent, concentration, and temperature. The most reliable hypotheses about the structural relaxation accompanying CT are those of a planar intramolecular CT state (PICT)[31] or a twisted intramolecular CT state (TICT).[32] In the present case, flexibility resides in the single bond linking the 6′-substituent to the molecular structure. Somewhat similar results were obtained by others[33] for spironaphthooxazines having electron-donor substituents; therein bathochromic shifts of fluorescence were connected to the electronic character of substituents as well as to the possible presence of new electronic n,π* transitions.

Because it has been proved for this[34] and related molecules[19,35] that the photoreaction SO → PM occurs at the singlet excited level on the time scale of picoseconds, whereas the fluorescence lifetimes are on the order of magnitude of nanoseconds,[36] it can be concluded that the reactive state is different from the fluorescent states.
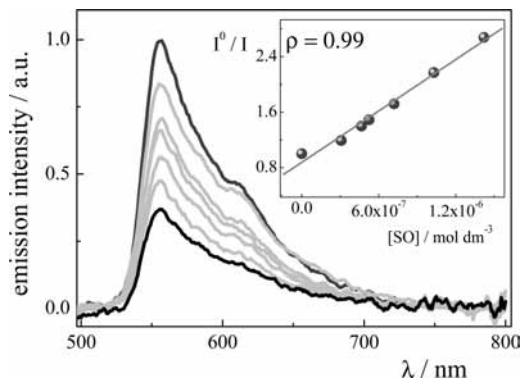
Photochromic Spirooxazine Excited-State Properties

J. Phys. Chem. A, Vol. 113, No. 34, 2009 **9429**
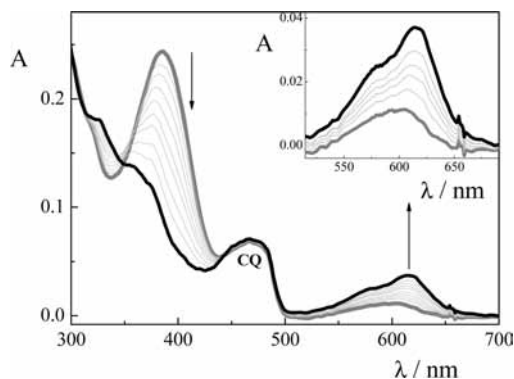

Figure 7. Spectral evolution of an ACN solution of SO (3.44×10^{-5} mol dm^{-3}) and CQ (3.54×10^{-3} mol dm^{-3}) upon continuous monochromatic irradiation with 450 nm light at 270 K. Inset: Zoom in the visible region; note the shift of the color band from 601 to 616 nm.
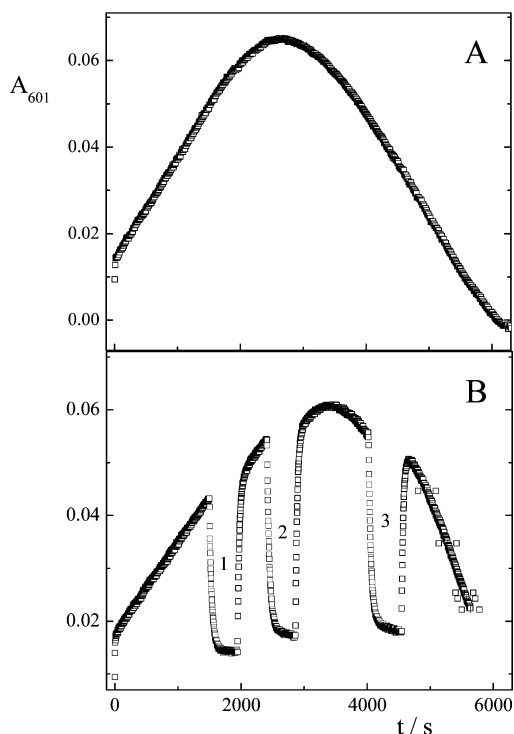

Figure 8. Kinetic profile of the color band ($\lambda_{anal} = 601$ nm, $\lambda_{exc} = 450$ nm, $T = 270$ K) developed by a 3.44×10^{-5} mol dm^{-3} ACN solution of SO upon irradiation of the photosensitizer ([CQ] $= 3.54 \times 10^{-3}$ mol dm^{-3}). (A) Continuous irradiation and (B) cycles of coloration and thermal bleaching.

$= 616$ nm). At the same time, a progressive decrease in intensity of the SO band at 386 nm (assigned to excitation localized into the naphthooxazine moiety) was observed, up to its complete disappearance and replacement by a weaker absorption at shorter wavelength ($\lambda_{max} \approx 358$ nm). Further prolonging the irradiation, the intensity of the color band at the photostationary state, as well as that of the new band in the UV region, decreased until both disappeared, with complete destruction of the photochromic functionality. The temporal evolution of the absorbance at 601 nm upon continuous irradiation of the photosensitizer is shown in Figure 8A. We carried out consecutive photocoloration/thermal bleaching cycles under the same experimental conditions by switching off the irradiation and then leaving the solution to thermally equilibrate in the dark from time to time (Figure 8B).

TABLE 3: Kinetic Parameters Determined for the Cycles of Photocoloration and Thermal Bleaching in the SO/CQ System in ACN at 270 K[a]

cycle	bleaching time/s	R^2	rise time/s	R^2
1	39.5 ± 0.5	0.998	30.1 ± 0.4	0.998
2	39.4 ± 0.3	0.999	31.9 ± 0.3	0.999
3	39.4 ± 0.3	0.999	24.1 ± 0.3	0.999

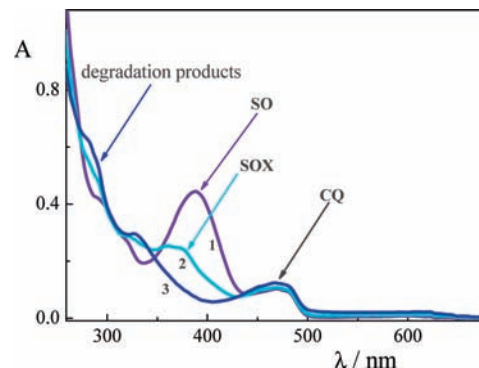[a] R^2 is the square correlation factor of the monoexponential fit.

Figure 9. Absorption spectra of prevailing deactivated forms: SO (1), SOX (2), and degradation products (3) in the ACN solution containing CQ.

From the on–off cycles, we obtained kinetic parameters, such as rise times of photocoloration and decay times of thermal bleaching, by fitting the curves with monoexponential functions in the 1500–4700 s time interval (cycles 1, 2, and 3). Below this interval, a fast rise was observed within the very first few seconds ($\sim$4 s), and above this interval, photobleaching apparently occurred. All kinetic data are presented in Table 3.

From all of the above, the following statements can be made. (1) Two distinct sensitized photochromic processes occurred. The first one, which was very fast, was replaced in a few seconds by a slower one. (2) After about 1000 s of total irradiation, only the slower process was observed with risetime stabilized around a constant value, $\sim$30 s, and bleaching at 39.5 s (corresponding to $k_\Delta = 0.0254$ s^{-1}), at any time the irradiation was interrupted (Table 2). Note that at the same temperature (270 K), the kinetic parameter ($k_\Delta = 0.16$ s^{-1})[6] of the PM produced by direct irradiation of SO is definitely different. (3) The spectrum of the colored form, after the initial fast process, was different from that obtained initially as well as by direct irradiation, showing a bathochromic shift from 601 to 616 nm (Figure 7), which was also different from the spectrum recorded after thermal bleaching (Figure 9). (4) There exists a photochromic molecule, SOX, that photoisomerizes to a colored merocyanine, PMX, whose absorption spectra are different from those of the original SO and PM. (5) Reproducible first-order kinetics in each cycle for both coloration and decoloration processes, within a wide time interval and under the adopted experimental conditions, indicate that the spectral and dynamic behavior is essentially dominated by the photosensitized photochromic process of the new molecular species SOX. (6) The new photochromic system undergoes degradation to byproduct(s) that do not absorb in the visible (Figure 9). (7) All photoprocesses, included degradation, are triggered by ^{3}CQ because CQ is the only species that absorbs the monochromatic (450 nm) irradiation light. (It was controlled that the minimal fraction of light absorbed by SO, not by SOX, did not detectably contribute to the overall photochemical processes.)
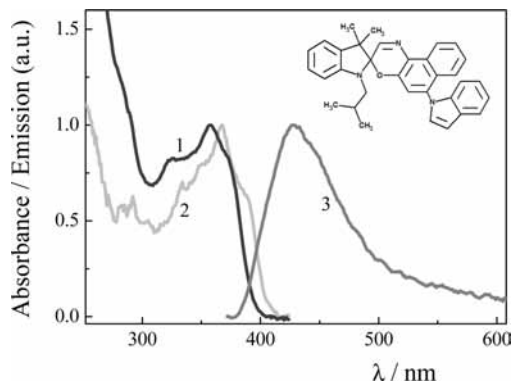
Figure 10. Normalized absorption (1), fluorescence excitation, $\lambda_{em} =$ 420 nm (2), and fluorescence emission, $\lambda_{exc} = 358$ nm (3) spectra of SOX in ACN at room temperature. Inset: Structure of SOX.
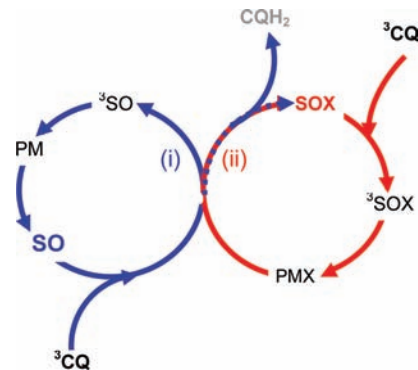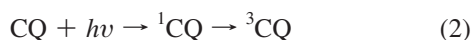

Figure 11. Schematic representation of the two-way interaction of ^{3}CQ with SO. Blue cycle (i) and blue arrows involve the SO/PM system. Red cycle (ii) describes processes implicating the SOX/PMX system.

The questions are now: What is the structure of the new photochromic system? By which mechanism is it formed? What is the mechanism of degradation ?

3.2.2. Photosensitized Reaction: Spectral Properties of SOX. In spectrum 2 of Figure 9, the typical band at 380 nm that was assigned to a transition involving the indolyl substituent is missing. Therefore, we believe that in some reaction step, passing through triplet sensitization, some change occurred to the 6′-substituent without altering the spiranic structure responsible for the photochromism. This was confirmed in a side experiment wherein a significant amount of SOX was accumulated, separated by HPLC, and analyzed by NMR and mass spectrometry. The molecular structure resulting was that shown in Figure 10. In the same Figure, the absorption spectrum of SOX exhibits the lowest energy band with a maximum at 358 nm ($\varepsilon = 6000$ dm^3 mol^{-1} cm^{-1}), whereas the bathochromic band ($\lambda_{max} \approx 380$ nm) is no longer present. This was expected for such structure where the indolyl substituent was oxidized; therefore, its electron-donating power decreased. The new molecule was also weakly fluorescent (Figure 10). The fluorescence maximum is located at 428 nm and shows a Stokes shift that is about half (~4500 cm^{-1}) of that found for SO fluorescence. The quantum yield was significantly excitation-wavelength-dependent, being 6×10^{-3} at the excitation maximum wavelength (367 nm) and 3.6×10^{-3} when excited on the absorption maximum (358 nm). It further decreased at shorter wavelengths; at $\lambda_{exc} < 290$ nm, the emission was hardly detectable. All of the above signifies that electronic as well as vibronic effects are operative. Similar behavior has been previously observed for several photochromic compounds and was attributed to the competition between photoreaction and vibrational relaxation at each vibrational level of an electronically excited state.[37] This competition reduces the population of the $S_1(0)$ level, from where fluorescence occurs, by as much as the excitation energy is high. As a consequence, the fluorescence excitation spectrum is different from the absorption spectrum (Figure 10) because it loses intensity toward the short wavelength region.

3.2.3. Photosensitized Reaction: The Mechanism. Our interpretation of the above findings is based on the experimental evidence that the intersystem crossing of CQ is practically unitary;[18] therefore, the only significantly photoactive species is the ^{3}CQ formed by intersystem crossing from the excited singlet state (eq 2).

$$CQ + h\nu \rightarrow {}^1CQ \rightarrow {}^3CQ \qquad (2)$$

The sensitizer molecule in its excited triplet state interacts with SO in two ways: (i) via energy transfer (ET) with the formation of ^{3}SO and complete recovery of the ground state sensitizer, and (ii) via hydrogen abstraction (HA), with the formation of the oxidized form SOX and consumption of the sensitizer, presumably due to irreversible transformation into its reduced form, hydroxycamphor (CQH$_2$). Hydrogen atom abstraction by the triplet state of camphorquinone from amines is a well-known photoreaction[38–43] that has been exploited to initiate photopolymerizations. The quantum yield of CQ disappearance in Bz, when irradiated in the presence of amines, was found around 0.18.[43] Radicals from amines must be primarily produced via exciplex formation through electron transfer, followed by proton transfer to give a ketyl radical, CQH$^\bullet$.[43] The disproportionation of free radicals in the solution leads to the formation of hydroxy camphors, CQH$_2$. Such products have been observed in the photolysis of CQ in isopropyl alcohol solutions.[38,44] In the present case, photooxidation that occurs at the side substituent of the photochrome does not destroy the photochromic functionality but significantly changes chromatic and dynamic properties of the system.

The interaction SO–^{3}CQ triggers two photochromic cycles (see Figure 11). The first (i), via ET, generates ^{3}SO that yields the open colored form PM reverting thermally back to SO. The second cycle (ii) results from the formation, by HA, of SOX that in turn, interacting with ^{3}CQ, is activated to the triplet state (^{3}SOX) and then relaxes to its merocyanine form, PMX, that undergoes thermal bleaching to SOX. The reduced inactive form of the sensitizer, produced via HA, contributes no further to ET. However, being the concentration ratio of the initial SO to CQ on the order of 10^{-2}, the amount of the reduced form of the sensitizer, which cannot exceed that of the starting SO, was spectrophotometrically undetectable, and the light absorbed by CQ may be considered to remain practically constant. The experimental run described above and illustrated in Figures 7–9 revealed that, with the exclusion of the very first irradiation times, cycle ii dominated the overall photobehavior, and the SOX/PMX system became the only system responsible for the on–off color switching. On the basis of the scheme of Figure 11, this can be understood, considering that the first cycle, controlled by the bleaching rate of the thermal process PM → SO ($k_\Delta^{PM} = 0.16$ s^{-1}), is very fast. It provides at any instant a large amount of SO available for entering into cycle ii, which is slower because it is controlled by the slow bleaching rate of PMX ($k_\Delta^{PMX} = 0.0253$ s^{-1}). As SOX accumulates, it enters competi-

Photochromic Spirooxazine Excited-State Properties

J. Phys. Chem. A, Vol. 113, No. 34, 2009 **9431**

tion with SO for the triplet energy transfer from ^{3}CQ. The constancy of the bleaching time, determined over a wide time period, approximately between 2000 and 4000 s of irradiation (Table 3) under the experimental conditions adopted, indicates that the colored form was different and longer lived than that produced during the first reaction steps and that the effective triplet energy acceptor has become SOX.

As pointed out above, whereas ET here, as in other analogous cases,[14−18] occurs with rate constant $k_{ET} \approx 4 \times 10^9$ dm^3 mol^{-1} s^{-1}, k_{HA} is expected to be about one order of magnitude smaller.[42] The occurrence of HA has not been detected in the study carried out by Wilkinson and coworkers on merocyanine formation via triplet-state sensitization,[14] probably because they used pulsed techniques that did not allow the detections of events occurring over a time scale longer than microseconds or because they used sensitizers that were less prone to hydrogen abstraction.

3.2.4. Photosensitized Reaction: Photokinetic Study. Taking into account the fact that the photosensitized reactions of SO and SOX occur over different and easily separable time intervals, the quantum yields of the photosensitized production of both PM and PMX could be determined.

The color-forming rate of the triplet sensitized process is given by the kinetic eq 3[15−18]

$$dA_{PM}/dt = \Phi_{PM}^{Sens} \times \varepsilon_{PM} \times I_{CQ} - k_\Delta^{PM} \times A_{PM} \quad (3)$$

where Φ_{PM}^{Sens} is the quantum yield of photoreaction, ε_{PM} is the molar absorption coefficient of PM, and I_{CQ} is the intensity of the light absorbed by the sensitizer (1 cm path length) and can be expressed as a function of the total incident light, I^0 (einstein dm^{-3} s^{-1}), and the CQ absorbance at the exciting wavelength, A_{CQ}, which was constant during the whole process, $I_{CQ} = I^0 [1 - \exp(-2.3 A_{CQ})]$. Because of the constancy of the product $\Phi_{PM}^{Sens} \times \varepsilon_{PM} \times I_{CQ}$, eq 3 can be easily integrated in a closed form (eq 4)

$$A_{PM} = \frac{\Phi_{PM}^{Sens} \times \varepsilon_{PM} \times I_{CQ}}{k_\Delta^{PM}} \times (1 - e^{-k_\Delta t}) =$$

$$A_{PM}^\infty \times (1 - e^{-k_\Delta t}) \quad (4)$$

From the initial reaction steps, the sensitized quantum yield, Φ_{PM}^{Sens}, could be calculated (eq 5)

$$\Phi_{PM}^{Sens} = (dA_{PM}/dt)_{t\to 0}/\{\varepsilon_{PM} I^0 [1 - \exp(-2.3 A_{CQ})]\} \quad (5)$$

To obtain a reliable Φ_{PM}^{Sens} value of the primary sensitized process, namely, the photoproduction of the PM (cycle i), we had to exploit only a very short temporal range. To increase the sensitivity of measurements by slowing down the reaction, it was followed at low light intensity by reducing the irradiation band pass from 16 to 8 nm and filtering the exciting light through a gray filter (6.1% transmittance). By using the above equations, under conditions of total quenching of the triplet sensitizer by SO, we determined $\Phi_{PM}^{Sens} = 1.3 \pm 0.3$.

To obtain the quantum yield of the SOX-sensitized reaction, Φ_{PMX}^{Sens} (cycle ii), we used analogous equations and obtained $\Phi_{PMX}^{Sens} = 1.2 \pm 0.2$. Values of Φ^{Sens} close to unity were also found by Wilkinson for structurally related molecules.[14]

The photobehavior of the directly excited SOX was also investigated; an example of the time course of photocoloration
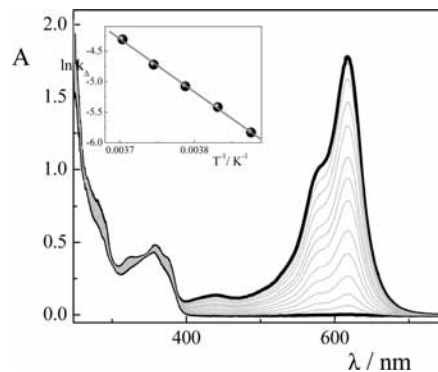

Figure 12. Spectral evolution of SOX in ACN solution irradiated at 358 nm at 248 K. Inset: Arrhenius plot for thermal bleaching.

is illustrated in Figure 12. The bathochromic shift of the color band of SOX, compared with that of SO, is in accord with the increased conjugation owing to the structure change. The quantum yield and molar absorption coefficient of the colored species were obtained using various previously developed methods,[6,45] and we determined the activation energy of the bleaching process by applying the Arrhenius equation in the 258−270 K temperature interval (Figure 12, inset). All photokinetic results are summarized in Table 4.

Calculation of activation parameters of the thermal bleaching of SOX (Table 5) by means of the Eyring equation indicates that the closing reaction is accompanied by a greater activation enthalpy and a less-negative activation entropy than that for SO. Both the increase in molecular constraints and the solvent reorganization around the polar transition state give a negative contribution to the activation entropy; the latter is smaller in the case of SOX/PMX system owing to its lower polar character.

The complementary influence on the thermal reaction of the energy and entropy factors results in almost unaltered activation free energy for the two molecules.

3.2.5. Photosensitized Reaction: Degradation. In the experiment described above and illustrated in Figure 8, degradation of the SOX/PMX system dominates the overall photosensitized process after about 4000 s of total irradiation. In the photodegradation process, a determining role is played by oxygen. In fact, by increasing the nitrogen flux and continuously maintaining the solution under the N$_2$ atmosphere during irradiation, the degradation was reduced. We hypothesize that it consists of a photooxidative interaction of SOX or PMX with some activated species of the residual oxygen still present even after bubbling the solution with nitrogen. There are two oxygen species that could be active, singlet oxygen, O$_2$($^1\Delta_g$), and superoxide radical anion, O$_2^{\bullet-}$.

Following the mechanism proposed by Guglielmetti, the singlet oxygen, O$_2$($^1\Delta_g$), attacks the ethenic double bond of the PM with formation of a dioxetane, which thermally evolves to the fragmentation products.[46]

An alternative proposal was suggested by Malatesta[47−50] that is based on the formation of the superoxide radical anion O$_2^{\bullet-}$ produced via a charge transfer process where the molecular oxygen acts as an acceptor and the excited merocyanine acts as a donor. Once produced in the primary step, O$_2^{\bullet-}$, which is a highly reactive nucleophilic species, attacks the radical cation of the merocyanine.

Under our experimental conditions, it was possible that ^{3}PMX was produced by CQ sensitization (eq 6a) and interacted with the molecular oxygen, yielding the radical cation PMX$^{\bullet+}$ and

TABLE 4: Photokinetic Results in ACN for the Directly Excited and Sensitized Photochromic Reactions

photochromic system	Φ^{dir}	Φ^{sens}	ε (dm³ mol⁻¹ cm⁻¹) (λ_{max}/nm)	k_Δ (270 K) (s⁻¹)	E_a (kJ mol⁻¹)	A (s⁻¹)
SO/PM	0.24,[a] 0.29[b]	1.3 ± 0.3	76 400[a] (601)	0.160	51[a]	1 × 10⁹
SOX/PMX	0.40	1.2 ± 0.2	29 600 (616)	0.0253	72	1 × 10¹²

[a] Data taken from ref 6. [b] Data taken from ref 14.

TABLE 5: Thermodynamic Activation Parameters of the Thermal Bleaching Reaction of PMX in ACN Compared with PM

photochromic system	$\Delta H^\ddagger$ (kJ mol⁻¹)	$\Delta S^\ddagger$ (J mol⁻¹ K⁻¹)	$\Delta G^\ddagger$ (kJ mol⁻¹)
SO/PM[a]	48.5	−80	72.2
SOX/PMX	68.5	−23	75.3

[a] Data taken from ref 6.

the radical anion, $O_2^{\bullet-}$ (eq 6b), which triggers the degradation (eq 6c)

$$PMX + {}^3CQ \rightarrow {}^3PMX + CQ \qquad (6a)$$

$$^3PMX + O_2({}^3\Sigma_g) \rightarrow PMX^{\bullet+} + O_2^{\bullet-} \qquad (6b)$$

$$PMX + O_2^{\bullet-} \rightarrow products \qquad (6c)$$

The interaction (eq 6a) could be made possible by the rather long lifetime of the newly produced PMX. It is in fact well known that the longer the lifetime of the metastable colored form, the shorter the durability of a photochrome.[49] Moreover, even if this molecule exhibits positive solvatochromism and therefore is less polar in the ground than in the excited state, a significant contribution of the zwitterionic form has been demonstrated to participate even in the ground-state structure,[49] which could allow the charge transfer interaction even in the ground state (eq 6b). The degradation mechanism proposed is also supported by literature findings that SOs and PMs do not produce $O_2({}^1\Delta_g)$ but are quenchers of $O_2({}^1\Delta_g)$;[47] therefore, the active oxygen species should be the radical anion, $O_2^{\bullet-}$.

4. Conclusions

In this work, the complicated array of the excited states of SO emerged. This molecule emitted from two different singlet excited states, an excited π,π^* state and an ICT state; the latter is stabilized in polar non-hydrogen-bonding solvents, resulting in the appearance of a low intensity bathochromic absorption band. Both excited states were reactive in producing the PM. Upon triplet sensitization, Φ_{PM}^{Sens} increased up to ~1. In addition to ET, the sensitizer also oxidized the photochrome by hydrogen abstraction from the 6′-substituent, thus generating a new photochromic molecule, here named SOX, which became competitive with SO in the interaction with ³CQ. The photocoloration of SOX was efficiently sensitized by CQ; $\Phi_{PMX}^{Sens} \approx 1$ versus direct $\Phi_{PMX} = 0.40$. The metastable photoproduced PMX had a longer lifetime than the original one, PM, and thus photocolorability increased but was also accompanied by photooxidative degradation, probably through interaction with the active species of oxygen, the superoxide anion, $O_2^{\bullet-}$. These results confirmed the fact that the presence of oxygen significantly affects the fatigue resistance of this class of materials and much more when the metastable colored form has a long lifetime. Even though the HA process is commonly observed

for the interaction of triplet excited carbonyl compounds and amines, it is new that such interaction transforms a photochromic molecule into a different photochrome, characterized by its own activation spectrum and a differently colored open form, as serendipitously observed in this work.

Supporting Information Available: NMR spectra. This material is available free of charge via the Internet at http://pubs.acs.org.

References and Notes

(1) (a) Hirshberg, Y. J.; Fisher, E. Low-temperature photochromism and its relation to thermochromism. *J. Chem. Soc.* **1953**, 629–636. (b) Hirshberg, Y. J.; Fisher, E. Photochromism and reversible multiple internal transitions in some spiropyrans at low temperatures, part II. *J. Chem. Soc.* **1954**, 3129–3137.

(2) Bercovici, T.; Heiligman-Rim, R.; Fisher, E. Photochromism in spiropyrans. VI. Trimethylindolinobenzospiropyran and its derivatives. *Mol. Photochem.* **1969**, *1*, 23–55.

(3) Guglielmetti, R. 4n + 2 Systems: Spiropyrans. In *Photochromism of Organic Compounds*; Dürr, H., Bouas-Laurent, H., Eds.; Elsevier: Amsterdam, The Netherlands, 1990; pp 314−466.

(4) Lokshin, V.; Samat, A.; Metelitsa, A. V. Spirooxazines: synthesis, structure, spectral, and photochromic properties. *Russ. Chem. Rev.* **2002**, *71*, 893–916.

(5) Maeda, S. Spirooxazines. In *Organic Photochromic and Thermochromic Compounds*; Crano, J. C., Guglielmetti, R. J., Eds.; Kluwer Academic/Plenum Publishers: New York, 1999; Vol. 1, pp 85−109.

(6) di Nunzio, M. R.; Gentili, P. L.; Romani, A.; Favaro, G. Photochromic, thermochromic and fluorescent spirooxazines and naphthopyrans: a spectrokinetic and thermodynamic study. *ChemPhysChem.* **2008**, *9*, 768–775.

(7) (a) Förster, Th. Transfer mechanisms of electronic excitation. *Discuss. Faraday Soc.* **1959**, *27*, 7–17. (b) Birks, J. B. *Photophysics of Aromatic Molecules*; John Wiley & Sons: New York, 1970.

(8) (a) Wilkinson, F. Electronic energy transfer between organic molecules in solution. *Adv. Photochem.* **1964**, *3*, 241–268. (b) Turro, N. J. Energy transfer processes. *Pure Appl. Chem.* **1977**, *49*, 405–429. (c) Lamola, A. A. Applications of electronic energy transfer in solution. *Photochem. Photobiol.* **1968**, *8*, 601–616. (d) Speiser, S. Novel aspects of intermolecular and intramolecular electronic energy transfer in solution. *J. Photochem.* **1983**, *22*, 195–211.

(9) Bach, H.; Calvert, J. G. Primary photochemical processes in the 366 nm photolysis of 5′,7′-dichloro-6′-nitro-1,3,3-trimethylindolinobenzopyrylospiran in acetonitrile. *J. Am. Chem. Soc.* **1970**, *92*, 2608–2614.

(10) Appriou, P.; Guglielmetti, R.; Garnier, F. Study of the photochemical processes in the benzopyranic ring opening reaction of photochromic spiropyrans. *J. Photochem.* **1978**, *8*, 145–165.

(11) Sakuragi, M.; Aoki, K.; Tamaki, T.; Ichimura, K. The role of triplet state of nitrospiropyran in their photochromic reaction. *Bull. Chem. Soc. Jpn.* **1990**, *63*, 74–79.

(12) (a) Eloy, D.; Escaffre, P.; Gautron, R.; Jardon, P. Sensitized photocoloration by triplet-triplet energy transfer of spirooxazines. *J. Chim. Phys.* **1992**, *89*, 897–914. (b) Eloy, D.; Gay, C.; Jardon, P. Mechanism of

Photochromic Spirooxazine Excited-State Properties

J. Phys. Chem. A, Vol. 113, No. 34, 2009 **9433**

photodegradation of a spirooxazine. Effects of the solvent, oxygen, DABCO, and photosensitization. *J. Chim. Phys. Phys.–Chim. Biol.* **1997**, *94*, 683–706.

(13) Kellmann, A.; Tfibel, F.; Pottier, E.; Guglielmetti, R.; Samat, A.; Rajzmann, M. Effect of nitro substituents on the photochromism of some spiro[indolinenaphthopyrans] under laser excitation. *J. Photochem. Photobiol., A* **1993**, *76*, 77–82.

(14) Hobley, J.; Wilkinson, F. Photochromism of naphthoxazine-spiro-indolines by direct excitation and following sensitisation by triplet-energy donors. *J. Chem. Soc., Faraday Trans.* **1996**, *92*, 1323–1330.

(15) Favaro, G.; Malatesta, V.; Mazzucato, U.; Ottavi, G.; Romani, A. Triplet reactivity of spiro indolino oxazines studied by photosensitization. *Mol. Cryst. Liq. Cryst.* **1994**, *246*, 299–302.

(16) Favaro, G.; Malatesta, V.; Miliani, C.; Romani, A. Photosensitization of photochromism of spiro-indoline-oxazines by camphorquinone. *J. Photochem. Photobiol., A* **1996**, *97*, 45–52.

(17) Favaro, G.; Mazzucato, U.; Ottavi, G.; Becker, R. S. Kinetic analysis of the photochromic behavior of a naturally occurring chromene (lapachenole) under steady irradiation. *Mol. Cryst. Liq. Cryst.* **1997**, *298*, 137–144.

(18) Romani, A.; Favaro, G.; Masetti, F. Luminescence properties of camphorquinone at room temperature. *J. Lumin.* **1995**, *63*, 183–188. and references therein.

(19) Gentili, P. L.; Danilov, E.; Ortica, F.; Rodgers, M. A.; Favaro, G. Dynamics of the excited states of chromenes studied by fast and ultrafast spectroscopies. *Photochem. Photobiol. Sci.* **2004**, *3*, 886–891.

(20) Ortica, F.; Moustrou, C.; Berthet, J.; Favaro, G.; Samat, A.; Guglielmetti, R.; Vermeersch, G.; Mazzucato, U. Comprehensive photo-kinetic and NMR study of a bi-photochromic supermolecule involving two naphthopyrans linked to a central thiophene unit through acetylenic bonds. *Photochem. Photobiol.* **2003**, *78*, 558–566.

(21) Dawson, W. R.; Windsor, M. W. Fluorescence yields of aromatic compounds. *J. Phys. Chem.* **1968**, *72*, 3251–3260.

(22) (a) Baerends, E. J.; Ellis, D. E.; Ros, P. Self-consistent molecular Hartree–Fock–Slater calculations. I. The computational procedure. *Chem. Phys.* **1973**, *2*, 41–51. (b) te Velde, G.; Baerends, E. J. Numerical integration for polyatomic systems. *J. Comput. Phys.* **1992**, *99*, 84–98. (c) Fonseca Guerra, C.; Snijders, J. G.; te Velde, G.; Baerends, E. J. Towards an order-N DFT method. *Theor. Chem. Acc.* **1998**, *99*, 391–403.

(23) Vosko, S. H.; Wilk, L.; Nusair, M. Accurate spin-dependent electron liquid correlation energies for local spin density calculations: a critical analysis. *Can. J. Phys.* **1980**, *58*, 1200–1211.

(24) Becke, A. Density-functional exchange-energy approximation with correct asymptotic behavior. *Phys. Rev. A* **1988**, *38*, 3098–3100.

(25) (a) van Gisbergen, S. J. A.; Snijders, J. G.; Baerends, E. J. Implementation of time-dependent density functional response equations. *Comput. Phys. Commun.* **1999**, *118*, 119–138. (b) van Gisbergen, S. J. A.; Snijders, J. G.; Baerends, E. J. A density functional theory study of frequency-dependent polarizabilities and van der Waals dispersion coefficients for polyatomic molecules. *J. Chem. Phys.* **1995**, *103*, 9347–9354.

(26) Dimroth, K.; Reichardt, C.; Siepmann, T.; Bohlmann, F. Pyridinium *N*-phenolbetaines and their use for the characterization of the polarity of solvents. *Liebigs Ann. Chem.* **1963**, *661*, 1–37.

(27) (a) Schneider, S.; Baumann, F. Photochromism of spirooxazines. I. Investigation of the primary processes in the ring-opening reaction by picosecond time-resolved absorption and emission spectroscopy. *Ber. Bunsen–Ges Phys Chem* **1987**, *91*, 1222–1224. (b) Schneider, S.; Baumann, F. Photochromism of spirooxazines. II. CARS-investigation of solvent effects on the isomeric distribution. *Ber. Bunsen–Ges Phys Chem* **1987**, *91*, 1225–1228.

(28) Favaro, G.; Masetti, F.; Mazzucato, U.; Ottavi, G.; Allegrini, P.; Malatesta, V. Photochromism, thermochromism and solvatochromism of some spiroindolinooxazine–photomerocyanine systems: effects of structure and solvent. *J. Chem. Soc., Faraday Trans.* **1994**, *90*, 333–338.

(29) Wojtyk, J. T. C.; Wasey, A.; Kazmaier, P. M.; Hoz, S.; Buncel, E. C. Thermal reversion mechanism of *N*-functionalized merocyanines to spiropyrans: a solvatochromic, solvatokinetic, and semiempirical study. *J. Phys. Chem. A* **2000**, *104*, 9046–9055.

(30) See, for example, Grabowski, Z. R.; Rotkiewicz, K.; Rettig, W. Structural changes accompanying intramolecular electron transfer: focus on twisted intramolecular charge-transfer states and structures. *Chem. Rev.* **2003**, *103*, 3899–4031, and references therein.

(31) Zachariasse, K. A. Comment on "Pseudo–Jahn–Teller and TICT-models: a photophysical comparison of *meta*- and *para*-DMABN derivatives" [*Chem. Phys. Lett.* **1999**, *305*, 8]. The PICT model for dual

fluorescence of aminobenzonitriles. *Chem. Phys. Lett.* **2000**, *320*, 8–13. (b) Il'ichev, Y. V.; Kühnle, W.; Zachariasse, K. A. Intramolecular charge transfer in dual fluorescent 4-(dialkylamino)benzonitriles. Reaction efficiency enhancement by increasing the size of the amino and benzonitrile subunits by alkyl substituents. *J. Phys. Chem. A* **1998**, *102*, 5670–5680.

(32) (a) Siemiarczuk, A.; Grabowski, Z. R.; Krówczyski, A.; Asher, M.; Ottolenghi, M. Two emitting states of excited *p*-(9-anthryl)-*N,N*-dimethylaniline derivatives in polar solvents. *Chem. Phys. Lett.* **1977**, *51*, 315–320. (b) Grabowski, Z. R.; Rotkiewicz, K.; Siemiarczuk, A. Dual fluorescence of donor–acceptor molecules and the twisted intramolecular charge transfer (TICT) states. *J. Lumin.* **1979**, *18/19*, 420–424.

(33) Luchina, V. G.; Sychev, I. Yu.; Shienok, A. I.; Zaichenko, N. L.; Marevtsev, V. S. Photochromism of spironaphthooxazines having electron-donor substituents. *J. Photochem. Photobiol., A* **1996**, *93*, 173–178.

(34) Wilkinson, F.; Worrall, D. R.; Hobley, J.; Jansen, L.; Williams, S. L.; Langley, A. J.; Matousek, P. Picosecond time-resolved spectroscopy of the photocoloration reaction of photochromic naphthoxazine-spiro-indolines. *J. Chem. Soc., Faraday Trans.* **1996**, *92*, 1331–1336.

(35) Tamai, N. H.; Miyasaka, H. Ultrafast dynamics of photochromic systems. *Chem. Rev.* **2000**, *100*, 1875–1890, and reference therein.

(36) di Nunzio, M. R.; Gentili, P. L.; Romani, A.; Favaro, G. Photochromism of some spirooxazines and naphtopyrans in the solid state and in polymer film, to be submitted for publication.

(37) (a) Becker, R. S.; Dolan, E.; Balke, D. E. Vibronic effects in photochemistry. Competition between internal conversion and photochemistry. *J. Chem. Phys.* **1969**, *50*, 239–245. (b) Becker, R. S.; Pelliccioli, A. P.; Romani, A.; Favaro, G. Vibronic quantum effects in fluorescence and photochemistry. Competition between vibrational relaxation and photochemistry and consequences on photochemical control. *J. Am. Chem. Soc.* **1999**, *121*, 2104–2109. (c) Becker, R. S.; Favaro, G.; Romani, A.; Gentili, P. L.; Dias, F. M. B. Vibronic effects in pathways of photochemistry and vibrational relaxation. *Chem. Phys.* **2005**, *316*, 108–116.

(38) Monroe, B. M.; Weiner, S. A.; Hammond, G. S. Mechanisms of photochemical reactions in solution. II. Photoreduction of camphorquinone. *J. Am. Chem. Soc.* **1968**, *90*, 1913–1914.

(39) Jakubiak, J.; Allonas, X.; Fouassier, J.-P.; Sionkowska, A.; Andrzejewska, E.; Linden, L. A.; Rabek, J. F. Camphorquinone-amines photoinitiating systems for the initiation of free radical polymerization. *Polymer* **2003**, *44*, 5219–5226.

(40) Singh, A.; Scott, A. R.; Sopchyshyn, F. Flash photolysis of camphorquinone and biacetyl. *J. Phys. Chem.* **1969**, *73*, 2633–2643.

(41) Evans, T. R.; Leermakers, P. A. Emission spectra and excited-state geometry of α-diketones. *J. Am. Chem. Soc.* **1967**, *89*, 4380–4382.

(42) Allonas, X.; Fouassier, J.-P.; Angiolini, L.; Caretti, D. Excited-state properties of camphorquinone based monomeric and polymeric photoinitiators. *Helv. Chim. Acta* **2001**, *84*, 2577–2588.

(43) Mateo, J. L.; Bosch, P.; Lozano, A. E. Reactivity of Radicals Derived from Dimethylanilines in Acrylic Photopolymerization. *Macromolecules* **1994**, *27*, 7794–7799.

(44) Meinwald, J.; Klingele, H. O. Photochemical reactions of camphorquinone. *J. Am. Chem. Soc.* **1966**, *88*, 2071–2073.

(45) Ottavi, G.; Ortica, F.; Favaro, G. Photokinetic methods: a mathematical analysis of the rate equations in photochromic systems. *Int. J. Chem. Kinet.* **1999**, *31*, 303–313.

(46) Salemi, C.; Giusti, G.; Guglielmetti, R. J. Effect of photodegradation on the thermal bleaching rate constant of photochromic compounds in spiro[indoline-pyran] and spiro [indoline-oxazine] series. *J. Photochem. Photobiol., A* **1995**, *86*, 247–252.

(47) Malatesta, V.; Milosa, M.; Millini, R.; Lanzini, L.; Bortolus, P.; Monti, S. Oxidative degradation of organic photochromes. *Mol. Cryst. Liq. Cryst.* **1994**, *246*, 303–310.

(48) Malatesta, V. Degradation of organic photochromes: light-promoted and dark reactions. *Mol. Cryst. Liq. Cryst.* **1997**, *298*, 345–350.

(49) Malatesta, V. Photodegradation of organic photochromes. In *Organic Photochromic and Thermochromic Compounds*; Crano, J. C., Guglielmetti, R. J., Eds.; Kluwer Academic/Plenum Publishers: New York, 1999; pp 65–166.

(50) Malatesta, V.; Neri, C.; Wis, M. L.; Montanari, L.; Millini, R. Thermal and photodegradation of photochromic spiroindolinenaphthooxazines and -pyrans: reaction with nucleophiles. Trapping of the merocyanine zwitterionic form. *J. Am. Chem. Soc.* **1997**, *119*, 3451–3455.